Atmospheric Environment 105 (2015) 121–129

Contents lists available at ScienceDirect

Atmospheric Environment

journal homepage: www.elsevier.com/locate/atmosenv

Inverse modeling of past lead atmospheric deposition in South Greenland

Charly Massa [a], *, Fabrice Monna [b], Vincent Bichet [a], Émilie Gauthier [a], Rémi Losno [c], Hervé Richard [a]

[a] UMR CNRS 6249, Laboratoire Chrono-environnement, Université de Franche-Comté, 16 route de Gray, 25030 Besançon Cedex, France
[b] UMR CNRS 6298, ARTéHIS, Université de Bourgogne, 6 bd Gabriel, 21000 Dijon, France
[c] UMR CNRS 7583, LISA, Université Paris-Diderot, Université Paris Est-Créteil, 61 av du Gal de Gaulle, 94010 Créteil Cedex, France

HIGHLIGHTS

- We provide a new paleoenvironmental record of lead concentrations and lead isotopic compositions from southern Greenland.
- The geological background is not favorable to the direct determination of anthropogenic fluxes.
- We used inverse modeling to estimate anthropogenic lead deposition through time.
- The model is validated by the coherence of the results obtained from two independent records.

ARTICLE INFO

Article history:
Received 28 May 2014
Received in revised form
9 January 2015
Accepted 10 January 2015
Available online 12 January 2015

Keywords:
Greenland
Pollution
Lead stable isotopes
Inverse modeling
Lake
Peat

ABSTRACT

The aim of this study is to model atmospheric lead fluxes in two different paleoenvironmental records located in southern Greenland. Fifty five sediment samples collected from the Lake Igaliku sedimentary sequence were analyzed for lead and aluminum concentrations, and lead isotopic compositions. The second archive consists in a previously published dataset, obtained from a minerogenic peat deposit, located at Tasiusaq, 16 km northwest from Lake Igaliku. A flux model fitted to both dataset produces similar results, allowing past anthropogenic atmospheric deposition to be reconstructed. This original method can be easily adapted for other studies where natural inputs dominate over discrete anthropogenic inputs.

1. Introduction

Long considered as a pristine remote region, the Arctic is now regarded as impacted by landscape degradation (Massa et al., 2012a; Sandgren and Fredskild, 1991), long range atmospheric deposition of anthropogenic nitrogen (Holtgrieve et al., 2011), persistent organic pollutants (Malmquist et al., 2003), and by toxic trace metals (Bindler et al., 2001a, 2001b; Candelone et al., 1995; Liu et al., 2012; Michelutti et al., 2009; Murozumi et al., 1969; Rosman et al., 1997; Shotyk et al., 2005b; Zheng et al., 2007). The Arctic region is also undergoing major human impacts through the effects of the rapid current warming (Screen and Simmonds, 2010), which is attributed to anthropogenic greenhouse gas emission (Gillett et al., 2008). The combination of these anthropogenic global change processes (climate change, pollution, and land-use) is predicted to have profound ecological, socioeconomic, and cultural consequences (Callaghan et al., 2010; Post et al., 2009). Thereby, any long term records of anthropogenic contaminants are welcome to model future environmental changes in this vulnerable and sensible region.

Numerous studies have demonstrated that, at least since the Industrial Revolution, Arctic environments have been notably affected by anthropogenic Pb inputs (Candelone et al., 1995;

---

* Corresponding author. Present/permanent address: Department of Earth and Environmental Sciences, Lehigh University, Bethlehem, PA 18015, USA.

E-mail addresses: chm313@lehigh.edu (C. Massa), fabrice.monna@u-bourgogne.fr (F. Monna), vincent.bichet@univ-fcomte.fr (V. Bichet), emilie.gauthier@univ-fcomte.fr (É. Gauthier), losno@lisa.univ-paris12.fr (R. Losno), herve.richard@univ-fcomte.fr (H. Richard).

http://dx.doi.org/10.1016/j.atmosenv.2015.01.025
1352-2310/

Michelutti et al., 2009). Only a few studies have unambiguously and precisely documented periods antecedent to the 19th century (Liu et al., 2012; Marshall et al., 2009; Rosman et al., 1997; Zheng et al., 2007). Indeed, the Arctic region is far from any mining and metallurgical centers that operated in the past (Bindler, 2011), and their impacts were low by comparison with those from modern emissions. As a consequence, it is difficult to detect and to distinguish former inputs unequivocally from the natural background. Lead isotopic geochemistry has been recognized as a powerful tool, able to palliate, at least partly, the limitations mentioned above (Komárek et al., 2008; Renberg et al., 2002). The discriminating power of the isotopic tool is known to depend on three main factors: (*i*) the natural Pb content should be low, and as steady as possible in terms of concentrations and isotopic signature, (*ii*) the isotopic compositions of the potential sources must be known and constrained, and (*iii*) the isotopic signatures of the anthropogenic and natural contributions should be as contrasted as possible. As an example, although Sweden is distant from past emissions, evidences of lead pollution can be clearly recognized as early as 3500–3000 BP, because of high $^{206}\mathrm{Pb}/^{207}\mathrm{Pb}$ ratios (1.52 ± 0.18) and low Pb concentrations ($7 \pm 3\ \mu\mathrm{g\ g}^{-1}$) in pristine lake sediments (Brännvall et al., 1997).

Because they are featured by favorable reduced natural background, the only studies that provided compelling evidences of pre-industrial metal pollution in Greenland have been undertaken on ice cores (Hong et al., 1994, 1996; Rosman et al., 1997). In a study focusing on lake sediments from West Greenland, no significant changes in lead concentrations could be identified before the 18th century (Bindler et al., 2001b). However, as $^{206}\mathrm{Pb}/^{207}\mathrm{Pb}$ background ratio was extremely contrasted (1.365 ± 0.084) in respect to past anthropogenic inputs ($^{206}\mathrm{Pb}/^{207}\mathrm{Pb} < 1.18$), noticeable shifts of $^{206}\mathrm{Pb}/^{207}\mathrm{Pb}$ ratios, indicating the influence of exogenous lead, could be seen during pre-industrial times.

There is often an additional difficulty in working with lake sediments: the isotopic signature of natural lead is generally not steady along sedimentary records. This is especially true in Greenland because the wide geological heterogeneity of sediment sources, ranging from Archaean basement to Quaternary glacial deposits, could cause large natural fluctuations of $^{206}\mathrm{Pb}/^{207}\mathrm{Pb}$ ratios (Lindeberg et al., 2005). Such a situation is expected to cause uncertainties when calculating airborne lead pollution, or worst, to hamper its detection (Renberg et al., 2002).

In the present study, Pb concentrations and isotopic compositions were measured in sediments from Lake Igaliku, located in southern Greenland, to estimate the atmospheric input of anthropogenic lead and its origin through time. As lead background concentrations are high, with rather noisy $^{206}\mathrm{Pb}/^{207}\mathrm{Pb}$ ratios, an inverse model based on some assumptions about past lead inputs was applied. These results are treated together with previously published data from a minerotrophic mire located nearby (Shotyk et al., 2003). Such an approach recently succeeded in a well-constrained experimental soil plot archive for Pb concentration and isotopic ratios, and $^{137}\mathrm{Cs}$ (Monna et al., 2009; Semlali et al., 2004).

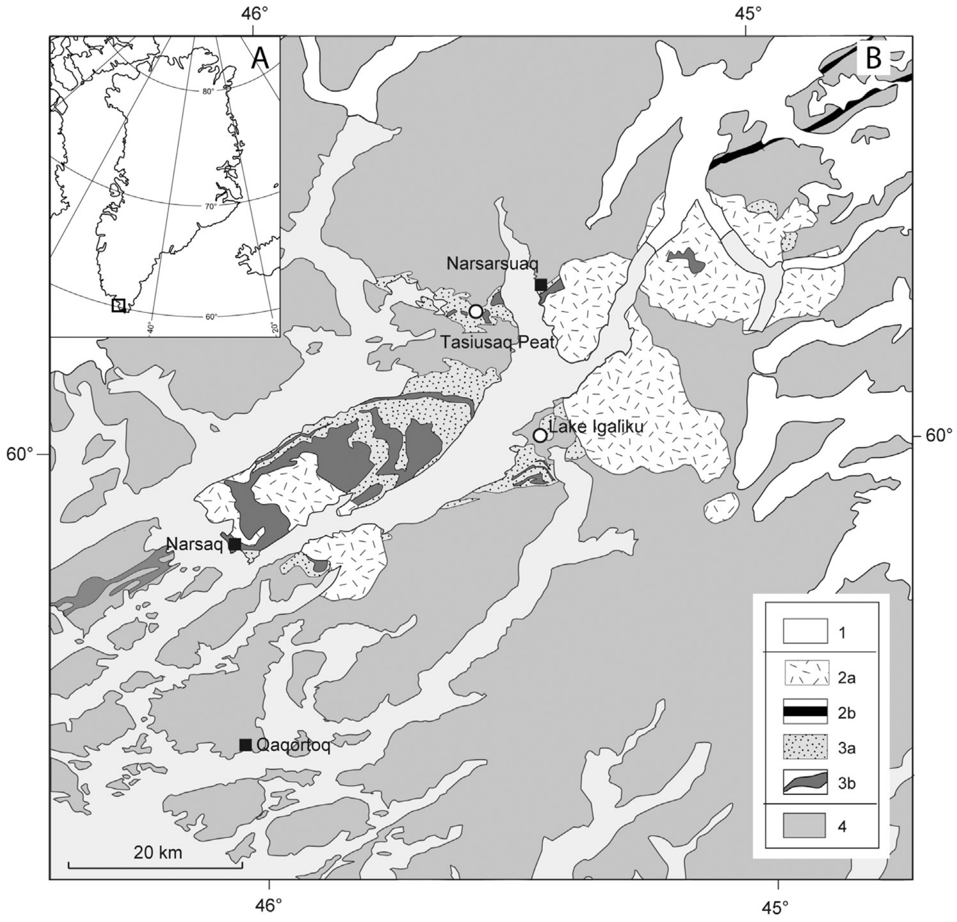

Fig. 1. A. Map of Greenland showing the location of the study area (boxed). B. Simplified geological map with the localization of Lake Igaliku and Tasiusaq peat of southern Greenland. 1- Inland ice; 2- Gardar intrusive rocks (a-syenite and nepheline–syenite complex; b-gabbro); 3- Eriksfjord formation (a-sandstone; b-basalt); 4- Julianehåb batholith (granite).

2. The site

The first archive is a sedimentary column sampled in Lake Igaliku (61°00.403′N, 45°26.494′W, Fig. 1). The lake occupies a low valley between the head of Igalikup Kangerlua (Igaliku Fjord) and Tunulliarfik (Erik's Fjord). The catchment area is 3.1 km^2, with relatively low relief. To the northeast, the slope ascends rather steeply to about 300 m a.s.l. The lake has a surface of 34 ha, a maximum depth of 26 m with one outflow but no major inflow. The second sequence is a peat deposit, located near the village of Tasiusaq (61°08.314′N, 45°33.703′W, Fig. 1), in an area characterized by rounded mountain topography, 16 km northwest from Lake Igaliku. It consists of a small circumneutral minerotrophic fen, probably formed through the terrestrialization of a shallow lake basin (Goodsite et al., 2002; Shotyk et al., 2003).

A wide variety of rocks, which may account for many natural Pb sources, can be found in the study region (Fig. 1). At Igaliku, the basement geology is mainly composed of the ~1.8 Ga old Julianehåb granite (Garde et al., 2002), unconformably overlain by sandstones interlayered with lavas, all forming the Eriksfjord formation. The catchment of the Tasiusaq peat consists exclusively in rocks belonging to the Eriksfjord formation (Andersen, 1997; Poulsen, 1964).

3. Material and methods

3.1. Sampling and geochemical analysis

Lake Igaliku. Details about fieldwork, sample preparation, measurements of water and organic carbon contents can be found in Massa et al. (2012a; 2012b). Briefly, the sediment core was sectioned into 0.5 cm intervals for the 10 uppermost cm and 1 cm intervals thereafter. Dry bulk density (DBD) was calculated from water content and wet bulk density measurements. For half of the samples, about 70 mg of powdered sediment were totally dissolved in Savillex® PTFE beakers on hot plate, using a tri-acid mixture of HCl, HNO_3 and HF of suprapure grade (Merck, Germany). The digested solutions were evaporated, retaken with HNO_3, diluted, and measured by a High Resolution Inductively Coupled Plasma – Mass Spectrometer (HR-ICP-MS) Thermo Element 2 for Pb, and by ICP-AES Spectro ARCOS, axial view, assisted by a CETAC ultrasonic nebulization for Al. Blanks and certified reference materials (CRMs): peach leaves NIST 1547, harbor sediment PACS-1, marine sediment BCSS-1, and basalt BCR-2, were systematically processed. Blanks were negligible with respect to the elemental composition of sediments, whereas values measured for CRMs did not differ from certified values by more than 10–15% for all elements considered. Three duplicates yielded similar concentrations, all within ±10%. Lead isotopic ratios ($^{206}Pb/^{207}Pb$ and $^{208}Pb/^{206}Pb$) were measured on selected samples using the same HR-ICP-MS. Mass bias was corrected by bracketing using a NBS 981 lead solution (Monna et al., 2000b, 1998). Accuracy was checked by measuring the BCR-2 certified reference material twice. Results ($^{206}Pb/^{207}Pb = 1.198 \pm 0.003$ and 1.200 ± 0.005; $^{208}Pb/^{206}Pb = 2.063 \pm 0.006$ and 2.067 ± 0.007; at 95% confidence level) are in good agreement with values previously measured using MC-ICPMS: $^{206}Pb/^{207}Pb = 1.2002–1.2007$ and $^{208}Pb/^{206}Pb = 2.0644–2.0651$ (Baker et al., 2004; Woodhead and Hergt, 2000).

Tasiusaq peat. Sampling, analytical procedures and results can be found in Goodsite et al. (2002) and Shotyk et al. (2003). Briefly, two replicate peat columns were contiguously analyzed for dry bulk density and 20 elemental concentrations including Pb, and for lead isotopic compositions on eight selected samples. Results were merged into a single master core.

3.2. Cores chronology

Lake Igaliku. The core chronology (Fig. 2a, Massa et al., 2012a) is based on 18 terrestrial macrofossil radiocarbon dates, and for the last 150 years, a 20-sample ^{137}Cs profile pointing out the maximum fallout consecutive to atmospheric nuclear weapon tests (1963 AD), and 14 ^{210}Pb measurements processed with a constant rate of supply model (Appleby and Oldfield, 1978). Radiocarbon measurements were calibrated using the northern hemisphere ^{14}C calibration dataset, Intcal09 (Reimer et al., 2009). The age–depth model was built using a cubic smooth spline function according to Blaauw (2010).

Tasiusaq peat. The post-1950 peat horizons have been accurately dated with 13 closely-spaced radiocarbon dates by using the atmospheric bomb pulse curve (Goodsite et al., 2002). Seven older samples were dated and calibrated in a classical way. The chronological data, initially reported in Shotyk et al. (2003), were retreated as for Igaliku. A sample at 36.5 cm depth was discarded because of its apparent incompatibility with the surrounding dates (Fig. 2b).

4. Results

4.1. Age-depth models

Lake Igaliku. The upper 120 cm of the core cover approximately the last 2700 years. The age-depth model is almost linear between ~700 BC and ~1000 AD (Fig. 2a) with an average sediment accumulation rate of 0.4 mm yr^{-1}. Then, the accumulation rate continuously rises to a maximum of ca. 0.8 mm yr^{-1}, around 1150 AD, and returns to its initial value, except during the 20th century where a sharp increase up to 1.9 mm yr^{-1} is noticed. The average uncertainty of the ^{14}C part of the model (below 15 cm) is ±100 yr, whereas the $^{210}Pb–^{137}Cs$ part of the model, corresponding to the 20th century when most of the lead pollution did occur, is very accurate with an error ranging between ± 25 yr in 1900 AD to ± 1.5 yr in 2000 AD.

Tasiusaq peat. The upper 90 cm of the peat column encompass approximately the last 3000 years. The peat growing rate tends to increase from the basis to the top (Fig. 2b): ~0.1 mm yr^{-1} before 1000 AD, ~0.3 mm yr^{-1} from 1000 AD, and 2.8 mm yr^{-1} for the 20th century. For the samples more recent than 1950 AD (above 20 cm), the high resolution ages obtained from the "atmospheric bomb pulse" calibration method are ± 3 yr. For the deeper layers, dated by the usual ^{14}C calibration method, the uncertainties are much greater (±110 yr).

4.2. Geochemical profiles

Lake Igaliku. The DBD is relatively steady with depth: ~0.33 g cm^{-3}, while Pb and Al concentrations oscillate around 13 µg g^{-1} and 6%, respectively (Fig. 2a). A common approach to identify anthropogenic contribution consists in normalizing Pb contents to those of a lithophilic element (Shotyk et al., 2001). Here, the normalized-Pb ratios were computed using Al (note that other lithophilic elements such as Zr, Ti or Sc could also be used in place). The Pb × 10,000/Al ratio profile appears to be smoother than those of Al or Pb taken separately, and rather stable around 2.2 ± 0.3 below 20 cm. The coefficient 10,000 is arbitrary here; it just makes more readable the ratio values. The $^{206}Pb/^{207}Pb$ ratios vary slightly around 1.276 ± 0.005 below 25 cm depth, and decrease upward to reach 1.230 at 6.75 cm, which is a turning point. Then, the $^{206}Pb/^{207}Pb$ ratios return sharply to the bottom values.

Tasiusaq peat. The DBD decreases upward: from 0.20 to 0.05 g cm^{-3} (Fig. 2b), as expected in such an organic-dominated environment. Pb concentrations vary smoothly between 1 and

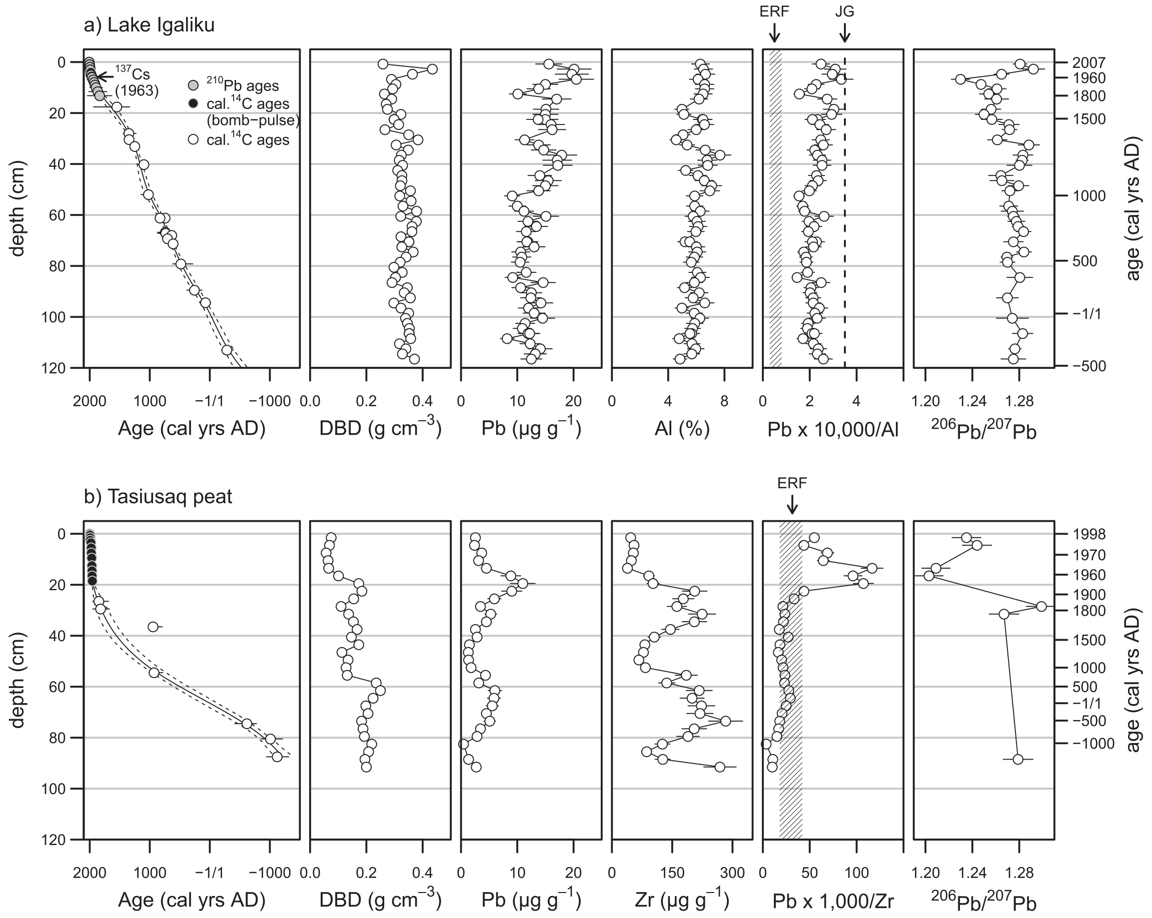

Fig. 2. Age-depth models with their 95% confidence limits (dashed lines), based on ^{137}Cs ^{210}Pb, ^{14}C and bomb pulse ^{14}C dates (arrow and grey, black or white filled circles respectively), dry bulk densities (DBD), lead, aluminium or zirconium concentrations, Pb × 10,000/Al or Pb × 1000/Zr ratios, ^{206}Pb/^{207}Pb ratios, and ages versus depth (left axis) and age (right axis) for the sequences of Lake Igaliku (this study) and Tasiusaq (data from Shotyk et al., 2003). The error bars represent a 95% confidence level. ERF (vertical hatched band) and JG (dashed line) refer to the compositions of the Eriksfjord and the Julianehåb rocks, respectively.

10 µg g^{-1}, with maximum concentrations found at approximately 20 cm depth. Below that depth, they are roughly correlated to those of Zr, which is used as normalizing element because Al was not measured by the authors of the study. Pb × 1000/Zr ratios are steady around 20 below 28 cm. Above, they consistently increase to reach a maximum value of 120 at ~16 cm depth. Only eight lead isotopic compositions are available for the Tasiusaq peat. They can be divided into two groups: the highest ^{206}Pb/^{207}Pb ratios beneath 20 cm, and a clear minimum value at 15–17 cm depth.

5. Discussion

5.1. Classical modeling

Basically, total lead concentration of the dry sample *i*, $Pb_{bulk}(i)$ expressed in µg g^{-1}, can be expressed as the sum of two components: (i) the natural one, $Pb_{nat}(i)$, and that (ii) the anthropogenic one, which results here from atmospheric deposition after long-range transport, $Pb_{anthr}(i)$:

$$Pb_{bulk}(i) = Pb_{nat}(i) + Pb_{anthr}(i) \tag{1}$$

Natural lead contribution in the *i* sediment sample can be estimated, assuming that natural lead is proportional to, say, aluminum content, as mentioned above:

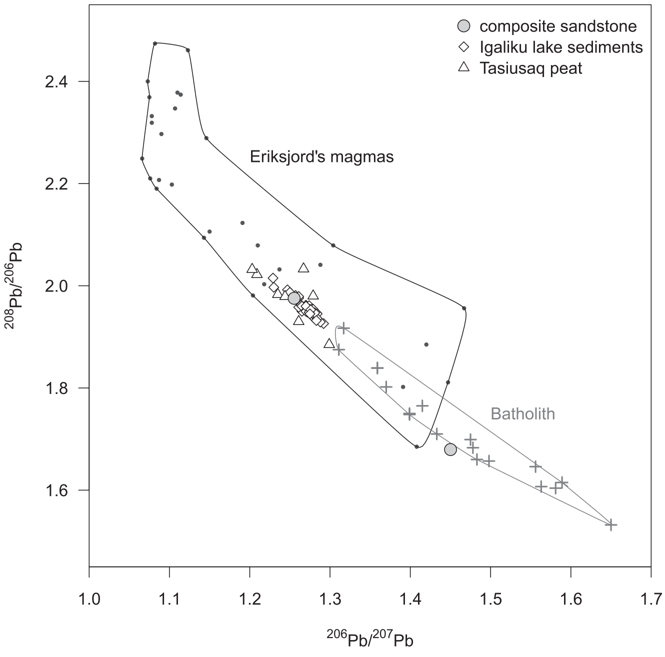

Fig. 3. ^{208}Pb/^{206}Pb vs. ^{206}Pb/^{207}Pb diagram. The Igaliku Lake sediment samples (open diamonds) and the Tasiusaq peat samples (open triangles) are represented together with the isotopic composition of endogenous lead: grey crosses, black dots, and grey filled circles correspond to samples from the Julianehåb granite, and from lavas and sandstones of the Eriksfjord formation respectively.

$$Pb_{nat}(i) = Al_{bulk}(i)\cdot(\mathrm{Pb/Al})_{\mathrm{back}} \tag{2}$$

where $Al_{bulk}(i)$ represents Al bulk concentration of the sample *i* and $(\mathrm{Pb/Al})_{\mathrm{back}}$ is the background ratio, assumed to be constant. Isotopically, the measured bulk $^{206}\mathrm{Pb}/^{207}\mathrm{Pb}$ ratio of any sample *i* can be approximated using a linear combination which involves two end-members: the isotopic composition of the natural component, supposed to be constant, $(^{206}\mathrm{Pb}/^{207}\mathrm{Pb})_{\mathrm{back}}$, and the overall anthropogenic component $(^{206}\mathrm{Pb}/^{207}\mathrm{Pb})_{\mathrm{anthr}}(i)$:

$$\left(\frac{^{206}\mathrm{Pb}}{^{207}\mathrm{Pb}}\right)_{bulk}(i) \approx \frac{Pb_{nat}(i)\left(\frac{^{206}\mathrm{Pb}}{^{207}\mathrm{Pb}}\right)_{\mathrm{back}} + Pb_{anthr(i)}\left(\frac{^{206}\mathrm{Pb}}{^{207}\mathrm{Pb}}\right)_{anthr}(i)}{Pb_{bulk}(i)} \tag{3}$$

The overall anthropogenic contribution and its isotopic signature are straightforwardly drawn by combining eqs. (1)–(3):

$$Pb_{anthr}(i) = Pb_{nat}(i) - Al_{bulk}(i)\cdot(Pb/Al)_{back} \tag{4}$$

$$\left(\frac{^{206}\mathrm{Pb}}{^{207}\mathrm{Pb}}\right)_{anthr}(i) \approx \frac{Pb_{bulk}(i)\left(\frac{^{206}\mathrm{Pb}}{^{207}\mathrm{Pb}}\right)_{bulk}(i) - Pb_{nat}(i)\left(\frac{^{206}\mathrm{Pb}}{^{207}\mathrm{Pb}}\right)_{\mathrm{back}}}{Pb_{anthr(i)}} \tag{5}$$

At Igaliku, the anthropogenic contribution, although present, is so low that it does not affect drastically the Pb × 10,000/Al ratios, except perhaps within the uppermost 20 cm (Fig. 2a). Shifts of isotopic compositions from the background values seem to be detected above ca. 25 cm depth, suggesting the presence of anthropogenic inputs. Such a sensitivity of isotopic compositions intrinsically ensues from the hyperbolic nature of the curve linking isotopic compositions to concentrations in case of binary mixing (see Faure, 1986 for theory and Monna et al., 2000a for an example).

The peat environment of Tasiusaq, even minerotrophic, is anticipated to be much more favorable than a lake sequence for calculating both $\mathrm{Pb_{anthr}}$ and $(^{206}\mathrm{Pb}/^{207}\mathrm{Pb})_{\mathrm{anthr}}$, because the material mainly consists in autochthonous organic matter and not in mineral matter naturally containing Pb, as in lake sediments. The signal-to-noise ratios, i.e. the anthropogenic over natural contributions, are therefore expected to be much higher when pollution did occur. Indeed, the rise of Pb × 1000/Zr from ~28 cm depth, concomitant with the sharp fall of the $^{206}\mathrm{Pb}/^{207}\mathrm{Pb}$ ratio (Fig. 2b), indicates a significant anthropogenic Pb fallout. Shotyk et al. (2003) considered this enrichment as low in comparison with a highly contaminated peat column from Denmark covering the same period.

In any case, the human-derived inputs are too low to calculate with a good precision the anthropogenic contributions and their isotopic compositions using eqs. (4) and (5). As an alternative, we propose in the following a new formulation to better constrain the model. Two new terms are introduced, and assumed to be reasonably known from the existing literature data: (i) the temporal evolution of Pb fallouts (not in terms of flux values, – it is the seek parameter -, but in terms of shape), and (ii) the overall isotopic composition of the anthropogenic emissions through time. Using these new constrains, a wide range of anthropogenic fluxes are considered, modeled concentrations and isotopic compositions are computed for each of them, and compared to what is really observed in natural archives. The best Pb flux history is reached when both Pb concentrations and isotopic compositions for modeled and observed values match.

5.2. New model formulation

Inside a 1 × 1 × 1 cm^3 of wet sediment the amount of lead of natural origin, $QPb_{nat}(i)$, is:

$$QPb_{nat(i)} = Pb_{nat}(i)\cdot m_{sol}(i) \tag{6}$$

where $m_{sol}(i)$ is the mass of solid contained in the sample *i*, which is equivalent, in that case, to the DBD. On the other hand, the amount of lead of anthropogenic origin, $QPb_{anthr}(i)$, is:

$$QPb_{anthr}(i) = \sum_{t=T}^{T+n} FPb_{anthr}(t) \tag{7}$$

where *T* and $T+n$ are the ages of the lower and upper limits of the sub-sample *i*, respectively, corresponding to a sediment accumulation during *n* years, and $FPb_{Anthr}(t)$ is the anthropogenic lead flux during the year *t*, expressed in μg cm^{-2} y^{-1}. The modeled bulk lead concentration of the sample *i*, $Pb_{modeled}(i)$, is calculated as follows:

$$Pb_{modeled}(i) = \frac{QPb_{nat}(i) + QPb_{anthr}(i)}{m_{sol}(i)} \tag{8}$$

Considering a conventional binary mixing, the modeled $^{206}\mathrm{Pb}/^{207}\mathrm{Pb}$ ratio of the sample *i* becomes:

$$\left(\frac{^{206}\mathrm{Pb}}{^{207}\mathrm{Pb}}\right)_{modeled}(i) \approx \frac{QPb_{nat}(i)\left(\frac{^{206}\mathrm{Pb}}{^{207}\mathrm{Pb}}\right)_{back} + \sum_{t=T}^{T+n}\left[FPb_{anthr}(t)\left(\frac{^{206}\mathrm{Pb}}{^{207}\mathrm{Pb}}\right)_{anthr}(t)\right]}{QPb_{nat}(i) + QPb_{anthr}(i)} \tag{9}$$

where the $(^{206}\mathrm{Pb}/^{207}\mathrm{Pb})_{anthr}(t)$ corresponds to the isotopic composition of the anthropogenic contribution alone deposited during the year *t*.

5.3. Feeding the model

Local background. The $(\mathrm{Pb/Al})_{\mathrm{back}}$ and $(^{206}\mathrm{Pb}/^{207}\mathrm{Pb})_{\mathrm{nat}}$ ratios are required to run the model. They can be obtained from the peat or sedimentary column given that pre-anthropogenic values are compatible with local catchment rocks. At Igaliku, Pb × 10,000/Al is 2.2 ± 0.3 below 20 cm depth (Fig. 2a). This value is consistent with a mixture of material deriving from the surrounding granites, lavas and sandstones: *i.e.* Pb × 10,000/Al = 0.3–0.8 ($n = 5$) reported for the Eriksfjord formation (ERF, Fig 2a) (Halama et al., 2003), and Pb × 10,000/Al = 3.5 ($n = 1$) found in the Julianehåb granite (JG, Fig 2a) (Kalsbeek and Taylor, 1985). For the Tasiusaq peat, Al was not reported, but published Zr concentrations can be used in place (Shotyk et al., 2003). The Pb × 1000/Zr = 20 below 28 cm match well the composition of the Eriksfjord formations (within 18–42, Halama et al., 2003) on which the peat developed (ERF, Fig. 2b).

Mean values calculated from the deepest horizons of the cores (below 28 cm and 25 cm for Tasiusaq and Igaliku respectively) appear therefore to be suitable as estimators of the local background, because the sedimentary processes tend to average natural inputs. Similar observations can be done for the isotopic compositions. Plotted in a ^{208}Pb/^{206}Pb *vs.* ^{206}Pb/^{207}Pb diagram (Fig. 3), local rocks exhibit a huge dispersion. The ^{206}Pb/^{207}Pb ratios of the Julianehåb granite vary widely from 1.31 to 1.65 ($n = 18$) (Andersen, 1997; Colville et al., 2011; Kalsbeek and Taylor, 1985). For the Eriksfjord formation, the range of variation is even greater: 1.07–1.47 ($n = 30$), reflecting its lithological heterogeneity (Andersen, 1997). Given that the contribution of each lithological source involved is susceptible to vary with time, the ^{206}Pb/^{207}Pb ratios observed in pre-anthropogenic horizons at both Igaliku (~1.26–1.29) and Tasiusaq (~1.28–1.29) appear to be particularly stable (Fig. 2a,b).

Anthropogenic lead flux and associated isotopic composition. Around Greenland, the atmospheric deposition history is expected to follow approximately the same pattern (Renberg et al., 2002; Shotyk et al., 1998), except close to eventual point sources. Interestingly, a well-dated salt mash record collected in West Iceland (Viðarhólmi, Fig. 4a), a little more than 1000 km eastward from Igaliku was continuously analyzed for Pb, Ti and stable lead isotopes (Marshall et al., 2009). Using Ti as a surrogate of the mineral matter, anthropogenic lead fluxes, $fPb_{anthr}(t)$, were obtained using the 1-2, 4 set of equations, while its isotopic composition, $(^{206}Pb/^{207}Pb)_{anthr}(t)$, was extracted using eq. (10):

$$\left(\frac{^{206}\mathrm{Pb}}{^{207}\mathrm{Pb}}\right)_{anthr}(t) \approx \frac{\left(\frac{^{206}\mathrm{Pb}}{^{207}\mathrm{Pb}}\right)_{bulk} \cdot \left(\frac{Pb}{Ti}\right)_{bulk} - \left(\frac{^{206}\mathrm{Pb}}{^{207}\mathrm{Pb}}\right)_{back} \cdot \left(\frac{Pb}{Ti}\right)_{back}}{\left(\frac{Pb}{Ti}\right)_{bulk} - \left(\frac{Pb}{Ti}\right)_{back}} \tag{10}$$

where the subscripts *back* and *anthr* denote the natural and anthropogenic fractions, and *bulk* the total. Our working hypothesis is that anthropogenic lead fluxes in southern Greenland, $FPb_{anthr}(t)$, can be assessed by multiplying the $fPb_{anthr}(t)$ function by a factor α (which is sought), representing an intensity adjustment:

$$FPb_{anthr}(t) = \alpha fPb_{anthr}(t) \tag{11}$$

5.4. Model fitting

To sum up, the set of equations modeling the evolution of Pb content and its isotopic composition in the sediments of Lake

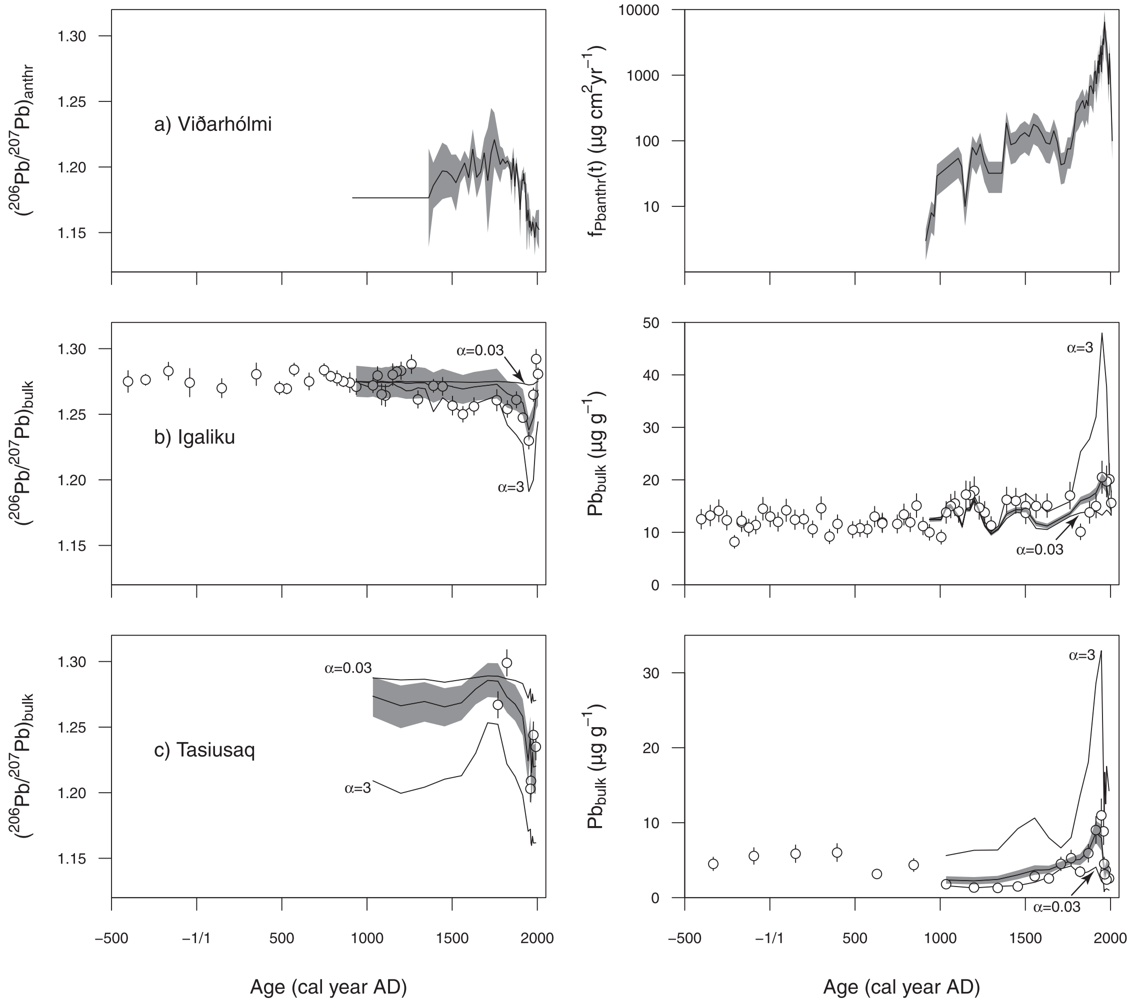

Fig. 4. Isotopic composition – $fPb_{anthr}(t)$ – and fluxes – ^{206}Pb/^{207}Pb$_{anthr}(t)$ – of anthropogenic lead reconstructed from the Icelandic record (Viðarhólmi). For Igaliku and Tasiusaq, modeled and measured Pb concentrations ^{206}Pb/^{207}Pb ratios are represented by grey bands (95% confidence envelopes) and closed circles, respectively. Modeled values for $\alpha = 0.03$ and 3 are also represented (without confidence envelope).

Table 1
Summary of the known data and unknowns used to run the model.

Parameter	Name	Value
Known variables		
bulk Al or Zr concentration of sample i	$Al\ or\ Zr_{bulk}(i)$	measured (Fig. 2)
bulk Pb concentration sediment of sample i	$Pb_{bulk}(i)$	measured (Fig. 2)
mass of solid contained in 1 cm^3 of sample i	$m_{Sol}(i)$	measured (Fig. 2)
bulk isotopic composition of sample i	$\left(\frac{^{206}Pb}{^{207}Pb}\right)_{bulk}(i)$	measured (Fig. 2)
age of the lower limit of sample i	T	computed from the age-depth models (Fig. 2)
age of the upper limit of sample i	$T+n$	
Input variables		
anthropogenic lead flux during the year t	$fPb_{anthr}(t)$	functions computed on the basis of literature values, using eqs. (1), (2), (4) and (10) (Fig. 4)
temporal evolution of isotopic composition of anthropogenic Pb	$\left(\frac{^{206}Pb}{^{207}Pb}\right)_{Anthr}(t)$	
Constants		
isotopic composition of endogenous Pb	$\left(\frac{^{206}Pb}{^{207}Pb}\right)_{back}$	Igaliku:1.275 ± 0.005[a] Tasiusaq: 1.285 ± 0.005[a]
Pb/Zr background ratio at Tasiusaq	$(Pb/Zr)_{back}$	20.6 ± 6.2[a]
Pb/Al background ratio at Igaliku	$(Pb/Al)_{back}$	2.14 ± 0.30[a]
Output values		
modeled total lead concentration in sample i	$Pb_{modeled}(i)$	eq. 8
modeled isotopic composition of bulk sediment of sample i	$\left(\frac{^{206}Pb}{^{207}Pb}\right)_{modeled}(i)$	eq. 9
Sought value		
coefficient applied to $fPb_{anthr}(t)$ to obtain annual fluxes in southern Greenland	α	eq. 11

[a] Deduced from measurements.

Igaliku and the Tasiusaq peat is governed by several variables and constants which are summarized in Table 1. The aim is (i) to let α vary within a reasonable range, (ii) to observe changes in terms of modeled Pb concentrations and isotopic compositions, (iii) to identify a domain of α which produces the best match between observed and modeled values and, (iv) to infer on historical lead deposition in southern Greenland.

For α varying from 0 to 3, with 0.01 increments, lead concentrations and isotopic compositions were computed following eqs. (6)–(9) and 11, by using the R software. Estimated errors on modeled values were obtained by a Monte Carlo procedure which generated 1000 samples for each parameter within their probability distribution. Optimal α values are reached by minimizing the sum of the squared differences between the observed and the computed values (fitting errors, *FEs*):

$$FE_{Pb} = \sum_{i=1}^{n} \left[Pb_{bulk}(i) - Pb_{modeled}(i)\right]^2 \tag{12}$$

$$FE_{iso} = \sum_{i=1}^{n} \left[\left(\frac{^{206}Pb}{^{207}Pb}\right)_{bulk}(i) - \left(\frac{^{206}Pb}{^{207}Pb}\right)_{modeled}(i)\right]^2 \tag{13}$$

When α is set to 0.01, the model matches approximately measured concentrations but clearly diverges for $^{206}Pb/^{207}Pb$ ratios at Igaliku (Fig. 4b), whereas both concentrations and $^{206}Pb/^{207}Pb$ ratios diverge at Tasiusaq (Fig. 4c). This can be explained by the lower natural lead content in the peat archive which makes it more sensitive to anthropogenic inputs. When $\alpha = 3$, simulations diverge strongly for both measured parameters at each site. If fluxes had been that high, $^{206}Pb/^{207}Pb$ ratios would have been much less radiogenic than measured, and concentrations would have peaked much higher. As expected, models deduced from isotopes are much more sensitive (i.e. clearer optimal α recognition) than those deriving from elemental concentrations. Given the degree of simplifications involved, the best matches are interestingly reached for comparable α values: between 0.20 and 0.59 for Tasiusaq, approximated at ~0.40 and between 0.52 and 0.61 for Igaliku, approximated at ~0.57 (Fig. 5). Such an overall similitude strongly pleads for the pertinence of our approach.

5.5. Inferences on historical lead deposition in southern Greenland

Evidences for pre-industrial lead pollution. At Igaliku, notable $^{206}Pb/^{207}Pb$ ratio shifts suggest that the first signs of anthropogenic inputs occurred in the 15th century (Fig. 4b). Similar observations were made by Liu et al. (2012) in the Svalbard archipelago (78.5°N). However, no Pb enrichment is detected in the Tasiusaq peat for the same period (Fig. 4c). Modeled $^{206}Pb/^{207}Pb$ ratios for the Tasiusaq peat sequence exhibit a clear decrease during the medieval period, suggesting that deeper and more closely spaced analyses of this sequence could have potentially allowed the detection, and even the quantification of a pre-industrial pollution signal.

Maximum anthropogenic lead fluxes. Anthropogenic lead fluxes are finally estimated by multiplying the $fPb_{\mathrm{anthr}}(t)$ function by the computed α values. Maximum anthropogenic fluxes of ~2400 ± 330 μg m^{-2} yr^{-1} are recorded in ca. 1965. They represent only 50% of what was atmospherically-deposited in Iceland (Marshall et al., 2009), 35% of that recorded in Faroe islands (Shotyk et al., 2005a), about 15% of the atmospheric fallout sampled in a Swiss peat bog, far from any direct source of pollution (Shotyk et al., 1998), and only ~7% of the anthropogenic lead fluxes assessed for Versailles, close to Paris, approximately at the same period (Semlali et al., 2004). This pattern is most likely driven by the distance from the major pollution sources. Similarly, the maximum Pb fallout decrease toward the North from Igaliku and Tasiusaq: 120–500 μg m^{-2} yr^{-1} in Western Greenland lakes for the early 1970s (Bindler et al., 2001b), 91 μg m^{-2} yr^{-1} at the Greenland PARCA Act2 site (McConnell et al., 2002), ~19 and ~39 μg m^{-2} yr^{-1} at Summit (Candelone et al., 1995) and Devon Island (Shotyk et al., 2005b) respectively. This decreasing pattern is, as above, due to the increasing distance to industrial sources, but also to the decreasing precipitation gradient with higher latitude and distance to the coast, which is known to partially control atmospheric lead fallouts (Bindler et al., 2001b). However, it cannot be ruled out that other factors, such as altitude, might have also contributed to that spatial pattern of atmospheric Pb depositions.

Lead pollution sources. The anthropogenic Pb recorded after the 1950s in Greenland ice is believed to derive mainly from a mixture of US and western European leaded gasoline, whose proportions have varied through time (Rosman et al., 1994, 1998). Further back in time, the situation is also complex because of the multiplicity of coal sources and lead ore deposits involved. Such an uncertainty about the primary sources of pollution could be an obstacle because the model needs proper knowledge of the $fPb_{anthr}(t)$ and $(^{206}Pb/^{207}Pb)_{anthr}(t)$ functions to run. These functions are likely different following the emission areas considered. For instance, lead in gasoline was banned in US almost 15 years before Europa, so that atmospheric Pb levels dropped earlier in Northern America (Rosman et al., 1994). Moreover, in the past, the massive use of lead deriving from Mississippi Valley Type ore deposits, characterized by highly radiogenic signatures ($^{206}Pb/^{207}Pb$ = 1.281–1.396) (Doe and Delevaux, 1972; Sangster et al., 2000) produced isotopic

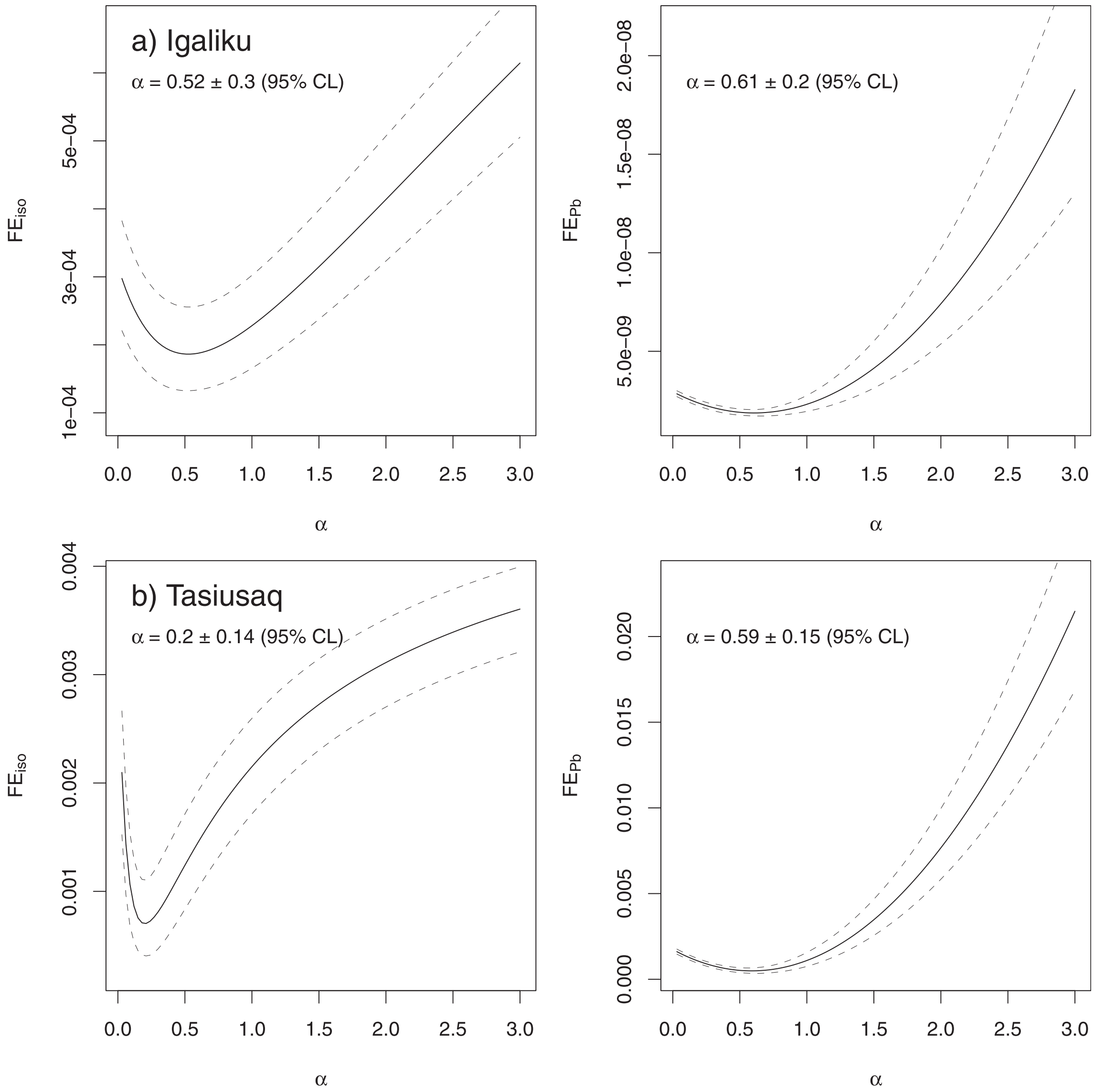

Fig. 5. Fitting errors for Pb concentrations (FE_{Pb}) and $^{206}Pb/^{207}Pb$ ratios (FE_{iso}) as functions of α. The dashed lines represent a confidence interval at 95%. The lower the FEs values, the better the concordance between modeled and measured data.

discrepancies between Northern America and Western Europe (Bindler et al., 2001b). Other major differences have also occurred before leaded gasoline was introduced as these areas did not experience the same industrial history. Our approach tends nonetheless to overcome all these difficulties because the $fPb_{anthr}(t)$ function is built here from a natural archive from Iceland, likely representative of the North Atlantic anthropogenic Pb fallout, notwithstanding their origin.

6. Conclusion

To the best of our knowledge, the present study constitutes the first application of inverse modeling for estimating anthropogenic lead pollution in paleoenvironmental records. The model is validated by the coherence of the results obtained from two profiles on two independent sequences. This method can be efficiently applied when the circumstances are not favorable to the direct determination of anthropogenic fluxes; in other terms when the human-derived inputs are difficult to decipher from the background. The main difficulty consists in finding reference curves of fluxes and isotopic compositions. This essential step must be adapted for each study region. By testing the model on two paleoenvironmental records in Southern Greenland, we estimated that anthropogenic lead fluxes did not exceed 2400 ± 330 $\mu g\ m^{-2}\ yr^{-1}$ (a maximum value recorded during the 1960s).

Acknowledgments

We would like to express our gratitude to Boris Vannière and Hervé Grisey for their help on the field and to Jean Lévèque and Olivier Mathieu for the easy access to the geochemical laboratory at the University of Burgundy. The study was funded by the Universities of Franche-Comté and Burgundy and the French Polar Institute (IPEV). This work is also partly supported by the French National Research Agency funded project ‘CEPS Greenland’ (ANR-10-CEPL-0008). Thanks also to Martine M Savard, François Lapointe and two anonymous reviewers for their insightful comments.

References

Andersen, T., 1997. Age and petrogenesis of the Qassiarsuk carbonatite-alkaline silicate volcanic complex in the Gardar rift, South Greenland. Mineral. Mag.

61, 499–513.

Appleby, P.G., Oldfield, F., 1978. The calculation of lead-210 dates assuming a constant rate of supply of unsupported ^{210}Pb to the sediment. Catena 5, 1–8.

Baker, J., Peate, D., Waight, T., Meyzen, C., 2004. Pb isotopic analysis of standards and samples using a 207Pb–204Pb double spike and thallium to correct for mass bias with a double-focusing MC-ICP-MS. Chem. Geol. 211, 275–303.

Bindler, R., 2011. Contaminated lead environments of man: reviewing the lead isotopic evidence in sediments, peat, and soils for the temporal and spatial patterns of atmospheric lead pollution in Sweden. Environ. Geochem. Health 33, 311–329.

Bindler, R., Renberg, I., Appleby, P.G., Anderson, N.J., Rose, N.L., 2001a. Mercury accumulation rates and spatial patterns in lake sediments from west Greenland: a coast to ice margin Transect. Environ. Sci. Technol. 35, 1736–1741.

Bindler, R., Renberg, I., John Anderson, N., Appleby, P.G., Emteryd, O., Boyle, J., 2001b. Pb isotope ratios of lake sediments in West Greenland: inferences on pollution sources. Atmos. Environ. 35, 4675–4685.

Blaauw, M., 2010. Methods and code for 'classical' age-modelling of radiocarbon sequences. Quat. Geochronol. 5, 512–518.

Brännvall, M.L., Bindler, R., Emteryd, O., Nilsson, M., Renberg, I., 1997. Stable isotope and concentration records of atmospheric lead pollution in peat and lake sediments in Sweden. Water, Air, Soil Pollut. 100, 243–252.

Callaghan, T.V., Bergholm, F., Christensen, T.R., Jonasson, C., Kokfelt, U., Johansson, M., 2010. A new climate era in the sub-Arctic: accelerating climate changes and multiple impacts. Geophys. Res. Lett. 37, L14705.

Candelone, J.-P., Hong, S., Pellone, C., Boutron, C.F., 1995. Post-industrial revolution changes in large-scale atmospheric pollution of the northern hemisphere by heavy metals as documented in central Greenland snow and ice. J. Geophys. Res. 100, 16605–16616.

Colville, E.J., Carlson, A.E., Beard, B.L., Hatfield, R.G., Stoner, J.S., Reyes, A.V., Ullman, D.J., 2011. Sr-Nd-Pb isotope evidence for ice-sheet presence on southern Greenland during the last interglacial. Science 333, 620–623.

Doe, B.R., Delevaux, M.H., 1972. Source of lead in Southeast Missouri Galena ores. Econ. Geol. 67, 409–425.

Faure, G., 1986. Principles of Isotope Geology. John Wiley and Sons, New York.

Garde, A.A., Chadwick, B., Grocott, J., Hamilton, M.A., McCaffrey, K.J.W., Swager, C.P., 2002. Mid-crustal partitioning and attachment during oblique convergence in an arc system, Palaeoproterozoic Ketilidian orogen, southern Greenland. J. Geological Soc. 159, 247–261.

Gillett, N.P., Stone, D.A., Stott, P.A., Nozawa, T., Karpechko, A.Y., Hegerl, G.C., Wehner, M.F., Jones, P.D., 2008. Attribution of polar warming to human influence. Nat. Geosci. 1, 750–754.

Goodsite, M.E., Heinemeier, J., Rom, W., Lange, T., Ooi, S., Appleby, P.G., Shotyk, W., van der Knaap, W.O., Lohse, C., Hansen, T.S., 2002. High resolution AMS ^{14}C dating of post bomb peat archives of atmospheric pollutants. Radiocarbon 43, 495–515.

Halama, R., Wenzel, T., Upton, B.G.J., Siebel, W., Markl, G., 2003. A geochemical and Sr-Nd-O isotopic study of the Proterozoic Eriksfjord Basalts, Gardar Province, South Greenland: reconstruction of an OIB signature in crustally contaminated rift-related basalts. Mineral. Mag. 67, 831–853.

Holtgrieve, G.W., Schindler, D.E., Hobbs, W.O., Leavitt, P.R., Ward, E.J., Bunting, L., Chen, G., Finney, B.P., Gregory-Eaves, I., Holmgren, S., Lisac, M.J., Lisi, P.J., Nydick, K., Rogers, L.A., Saros, J.E., Selbie, D.T., Shapley, M.D., Walsh, P.B., Wolfe, A.P., 2011. A coherent signature of anthropogenic nitrogen deposition to remote watersheds of the northern hemisphere. Science 334, 1545–1548.

Hong, S., Candelone, J.-P., Patterson, C.C., Boutron, C.F., 1994. Greenland ice evidence of hemispheric Lead pollution two millennia ago by Greek and Roman civilizations. Science 265, 1841–1843.

Hong, S., Candelone, J.-P., Patterson, C.C., Boutron, C.F., 1996. History of ancient copper smelting pollution during Roman and medieval times recorded in Greenland ice. Science 272, 246–249.

Kalsbeek, F., Taylor, P.N., 1985. Isotopic and chemical variation in granites across a Proterozoic continental margin—the Ketilidian mobile belt of South Greenland. Earth Planet. Sci. Lett. 73, 65–80.

Komárek, M., Ettler, V., Chrastný, V., Mihaljevič, M., 2008. Lead isotopes in environmental sciences: a review. Environ. Int. 34, 562–577.

Lindeberg, C., Bindler, R., Renberg, I., Emteryd, O., Karlsson, E., Anderson, N.J., 2005. Natural fluctuations of Mercury and Lead in Greenland Lake sediments. Environ. Sci. Technol. 40, 90–95.

Liu, X., Jiang, S., Zhang, P., Xu, L., 2012. Effect of recent climate change on Arctic Pb pollution: a comparative study of historical records in lake and peat sediments. Environ. Pollut. 160, 161–168.

Malmquist, C., Bindler, R., Renberg, I., van Bavel, B., Karlsson, E., Anderson, N.J., Tysklind, M., 2003. Time trends of selected persistent organic pollutants in Lake sediments from Greenland. Environ. Sci. Technol. 37, 4319–4324.

Marshall, W.A., Clough, R., Gehrels, W.R., 2009. The isotopic record of atmospheric lead fall-out on an Icelandic salt marsh since AD 50. Sci. Total Environ. 407, 2734–2748.

Massa, C., Bichet, V., Gauthier, É., Perren, B.B., Mathieu, O., Petit, C., Monna, F., Giraudeau, J., Losno, R., Richard, H., 2012a. A 2500 year record of natural and anthropogenic soil erosion in South Greenland. Quat. Sci. Rev. 32, 119–130.

Massa, C., Perren, B., Gauthier, É., Bichet, V., Petit, C., Richard, H., 2012b. A multiproxy evaluation of Holocene environmental change from Lake Igaliku, South Greenland. J. Paleolimnol. 48, 241–258.

McConnell, J.R., Lamorey, G.W., Hutterli, M.A., 2002. A 250-year high-resolution record of Pb flux and crustal enrichment in central Greenland. Geophys. Res. Lett. 29, 2130.

Michelutti, N., Simonetti, A., Briner, J.P., Funder, S., Creaser, R.A., Wolfe, A.P., 2009. Temporal trends of pollution Pb and other metals in east-central Baffin Island inferred from lake sediment geochemistry. Sci. Total Environ. 407, 5653–5662.

Monna, F., Hamer, K., Lévêque, J., Sauer, M., 2000a. Pb isotopes as a reliable marker of early mining and smelting in the Northern Harz province (Lower Saxony, Germany). J. Geochem. Explor. 68, 201–210.

Monna, F., Loizeau, J.-L., Thomas, B., Guéguen, C., Favarger, P.-Y., Losno, R., Dominik, J., 2000b. Noise identification and sampling frequency determination for precise Pb isotopic measurements by quadrupole-based inductively coupled plasma mass Spectrometry. Analusis 28, 750–757.

Monna, F., Loizeau, J.L., Thomas, B.A., Guéguen, C., Favarger, P.Y., 1998. Pb and Sr isotope measurements by inductively coupled plasma–mass spectrometer: efficient time management for precision improvement. Spectrochim. Acta B At. Spectrosc. 53, 1317–1333.

Monna, F., van Oort, F., Hubert, P., Dominik, J., Bolte, J., Loizeau, J.L., Labanowski, J., Lamri, J., Petit, C., Le Roux, G., Chateau, C., 2009. Modeling of ^{137}Cs migration in soils using an 80-year soil archive: role of fertilizers and agricultural amendments. J. Environ. Radioact. 100, 9–16.

Murozumi, M., Chow, T.J., Patterson, C., 1969. Chemical concentrations of pollutant lead aerosols, terrestrial dusts and sea salts in Greenland and Antarctic snow strata. Geochimica Cosmochimica Acta 33, 1247–1294.

Post, E., Forchhammer, M.C., Bret-Harte, M.S., Callaghan, T.V., Christensen, T.R., Elberling, B., Fox, A.D., Gilg, O., Hik, D.S., Høye, T.T., Ims, R.A., Jeppesen, E., Klein, D.R., Madsen, J., McGuire, A.D., Rysgaard, S., Schindler, D.E., Stirling, I., Tamstorf, M.P., Tyler, N.J.C., van der Wal, R., Welker, J., Wookey, P.A., Schmidt, N.M., Aastrup, P., 2009. Ecological dynamics across the arctic associated with recent climate change. Science 325, 1355–1358.

Poulsen, V., 1964. The sandstones of the precambrian eriksfjord formation in South Greenland. Rapp. Grønl. Geol. Under 2, 16.

Reimer, P.J., Baillie, M.G.L., Bard, E., Bayliss, A., Beck, J.W., Blackwell, P.G., Ramsey, C.B., Buck, C.E., Burr, G.S., Edwards, R.L., Friedrich, M., Grootes, P.M., Guilderson, T.P., Hajdas, I., Heaton, T.J., Hogg, A.G., Hughen, K.A., Kaiser, K.F., Kromer, B., McCormac, F.G., Manning, S.W., Reimer, R.W., Richards, D.A., Southon, J.R., Talamo, S., Turney, C.S.M., van der Plicht, J., Weyhenmeyer, C.E., 2009. IntCal09 and Marine09 radiocarbon age calibration curves, 0-50,000 years cal BP. Radiocarbon 51, 1111–1150.

Renberg, I., Brännvall, M.L., Bindler, R., Emteryd, O., 2002. Stable lead isotopes and lake sediments—a useful combination for the study of atmospheric lead pollution history. Sci. Total Environ. 292, 45–54.

Rosman, K.J.R., Chisholm, W., Boutron, C.F., Candelone, J.P., Hong, S., 1994. Isotopic evidence to account for changes in the concentration of lead in Greenland snow between 1960 and 1988. Geochimica Cosmochimica Acta 58, 3265–3269.

Rosman, K.J.R., Chisholm, W., Boutron, C.F., Candelone, J.P., Jaffrezo, J.L., Davidson, C.I., 1998. Seasonal variations in the origin of lead in snow at Dye 3. Greenl. Earth Planet. Sci. Lett. 160, 383–389.

Rosman, K.J.R., Chisholm, W., Hong, S., Candelone, J.-P., Boutron, C.F., 1997. Lead from Carthaginian and Roman Spanish mines isotopically identified in Greenland ice dated from 600 B.C. to 300 A.D. Environ. Sci. Technol. 31, 3413–3416.

Sandgren, P., Fredskild, B., 1991. Magnetic measurements recording late Holocene man-induced erosion in S. Greenland. Boreas 20, 315–331.

Sangster, D.F., Outridge, P.M., Davis, W.J., 2000. Stable lead isotope characteristics of lead ore deposits of environmental significance. Environ. Rev. 8, 115–147.

Screen, J.A., Simmonds, I., 2010. The central role of diminishing sea ice in recent Arctic temperature amplification. Nature 464, 1334–1337.

Semlali, R.M., Dessogne, J.B., Monna, F., Bolte, J., Azimi, S., Navarro, N., Denaix, L., Loubet, M., Chateau, C., van Oort, F., 2004. Modeling Lead input and output in soils using Lead isotopic geochemistry. Environ. Sci. Technol. 38, 1513–1521.

Shotyk, W., Goodsite, M.E., Roos-Barraclough, F., Frei, R., Heinemeier, J., Asmund, G., Lohse, C., Hansen, T.S., 2003. Anthropogenic contributions to atmospheric Hg, Pb and as accumulation recorded by peat cores from southern Greenland and Denmark dated using the 14C “bomb pulse curve”. Geochimica Cosmochimica Acta 67, 3991–4011.

Shotyk, W., Goodsite, M.E., Roos-Barraclough, F., Givelet, N., Le Roux, G., Weiss, D., Cheburkin, A.K., Knudsen, K., Heinemeier, J., van Der Knaap, W.O., Norton, S.A., Lohse, C., 2005a. Accumulation rates and predominant atmospheric sources of natural and anthropogenic Hg and Pb on the Faroe Islands. Geochimica Cosmochimica Acta 69, 1–17.

Shotyk, W., Weiss, D., Appleby, P.G., Cheburkin, A.K., Frei, R., Gloor, M., Kramers, J.D., Reese, S., Van Der Knaap, W.O., 1998. History of atmospheric Lead deposition since 12,370 14C yr BP from a peat bog, Jura mountains, Switzerland. Science 281, 1635–1640.

Shotyk, W., Weiss, D., Kramers, J.D., Frei, R., Cheburkin, A.K., Gloor, M., Reese, S., 2001. Geochemistry of the peat bog at Etang de la Gruère, Jura Mountains, Switzerland, and its record of atmospheric Pb and lithogenic trace metals (Sc, Ti, Y, Zr, and REE) since 12,370 14C yr BP. Geochimica Cosmochimica Acta 65, 2337–2360.

Shotyk, W., Zheng, J., Krachler, M., Zdanowicz, C., Koerner, R., Fisher, D., 2005b. Predominance of industrial Pb in recent snow and ice from Devon Island, Arctic Canada. Geophys. Res. Lett. 32, L21814.

Woodhead, J.D., Hergt, J.M., 2000. Pb-Isotope analyses of USGS reference materials. Geostand. Newsl. 24, 33–38.

Zheng, J., Shotyk, W., Krachler, M., Fisher, D.A., 2007. A 15,800-year record of atmospheric lead deposition on the Devon Island Ice Cap, Nunavut, Canada: natural and anthropogenic enrichments, isotopic composition, and predominant sources. Glob. Biogeochem. Cycles 21, GB2027.